



## RESEARCH LETTER

10.1002/2018GL077478

## Key Points:

- Different dynamical model cores can significantly affect simulations of Arctic winter climate and associated teleconnection in midlatitude
- A spectral element core on cubed-sphere grid simulates a warmer Arctic winter surface than a finite volume core on latitude-longitude grid
- The spectral element core simulates a robust cooling response over North America in the simulations forced by reduced Arctic sea ice cover

## Supporting Information:

- Supporting Information S1

## Correspondence to:

B.-M. Kim,  
bmkim@kopri.re.kr

## Citation:

Jun, S.-Y., Choi, S.-J., & Kim, B.-M. (2018). Dynamical core in atmospheric model does matter in the simulation of Arctic climate. *Geophysical Research Letters*, *45*, 2805–2814. <https://doi.org/10.1002/2018GL077478>

Received 28 NOV 2017

Accepted 28 FEB 2018

Accepted article online 5 MAR 2018

Published online 26 MAR 2018

## Dynamical Core in Atmospheric Model Does Matter in the Simulation of Arctic Climate

Sang-Yoon Jun<sup>1</sup> , Suk-Jin Choi<sup>2</sup> , and Baek-Min Kim<sup>1</sup>

<sup>1</sup>Korea Polar Research Institute, Incheon, South Korea, <sup>2</sup>Korea Institute of Atmospheric Prediction Systems, Seoul, South Korea

**Abstract** Climate models using different dynamical cores can simulate significantly different winter Arctic climates even if equipped with virtually the same physics schemes. Current climate simulated by the global climate model using cubed-sphere grid with spectral element method (SE core) exhibited significantly warmer Arctic surface air temperature compared to that using latitude-longitude grid with finite volume method core. Compared to the finite volume method core, SE core simulated additional adiabatic warming in the Arctic lower atmosphere, and this was consistent with the eddy-forced secondary circulation. Downward longwave radiation further enhanced Arctic near-surface warming with a higher surface air temperature of about 1.9 K. Furthermore, in the atmospheric response to the reduced sea ice conditions with the same physical settings, only the SE core showed a robust cooling response over North America. We emphasize that special attention is needed in selecting the dynamical core of climate models in the simulation of the Arctic climate and associated teleconnection patterns.

### 1. Introduction

Recent observations have shown that trends of declining Arctic sea ice and warming temperatures in the Arctic winter are intensifying especially in the current century (Stroeve et al., 2012; Walsh et al., 2017). On the other hand, in the midlatitude continental region of the Northern Hemisphere, where much of the world's population resides, there have been extreme winter cold events and a tendency of cooling down during this period (Van Oldenborgh et al., 2015; Wallace et al., 2014). The association of cooling trends in the continental Northern Hemisphere and the decline of Arctic sea ice and the warming of the Arctic region have recently emerged in a spatial pattern known as Warm Arctic, Cold Continents (Overland et al., 2011). These simultaneous climatic changes in the Arctic and midlatitudes are raising the need for accurate climate modeling and forecasting for the Arctic region.

However, it has also been reported that global climate modeling has uncertainties, including a mean bias with respect to observations and large diversity across models in the Arctic region (Intergovernmental Panel on Climate Change, 2014; Randall et al., 1998; Walsh et al., 2002). For example, a cold winter bias over the Arctic has been found in climate simulations such as the Coupled Model Intercomparison Project phase 3 (CMIP3) and phase 5 (CMIP5) (Intergovernmental Panel on Climate Change, 2014). Recent substantial declines in sea ice over the Arctic could not be captured by climate models (Rampal et al., 2011; Stroeve et al., 2012). The diversity of cloud cover among climate models has also been considerable in the Arctic in the CMIP3 and CMIP5 models (Karlsson & Svensson, 2011, 2013; Vavrus et al., 2009).

The modeling results for Warm Arctic, Cold Continents are also very diverse, making the causal relationship between the warm Arctic and cold continents controversial (Deser et al., 2016; Overland et al., 2016; Sun et al., 2016). Some studies suggest that declining sea ice in the Arctic region results in cooling of the midlatitude continental region, but other results suggest that Arctic sea ice loss does not induce cooling in the northern midlatitudes. For example, simulation results from Kim et al. (2014) suggested that reduced sea ice over the Kara-Barents Seas induced Eurasian cooling by weakening the polar vortex. Kug et al. (2015) found relationships between cold winters over North America/East Asia and sea ice reductions over the East Siberian/Barents-Kara Seas in CMIP5 multimodel simulations. However, in the multimodel ensemble experiments conducted by Sun et al. (2016), decreasing sea ice could not produce a cooling effect in the continental regions. Thus, the diversity of climate simulation results over the Arctic produces uncertainty regarding the relationship between Arctic and midlatitude teleconnection.

It has been suggested that these uncertainties in Arctic climate modeling are mainly linked to observational difficulties and consequent poor understanding of the relevant physical processes (Arctic Climate Impact

Assessment, 2005; Hodson et al., 2013). A large internal variability within atmospheric circulation systems over the Arctic also contributes to this relationship between observation and understanding. Accordingly, improvements in Arctic modeling have mainly been carried out by improving the presenting physical processes and reducing the diversity of modeling results (Hines et al., 2015; Vavrus & Waliser, 2008; Yao et al., 2016).

However, in addition to physical processes, the dynamical cores used in atmospheric models could play a key role in the uncertainty afflicting Arctic climate research. The dynamical core, which is responsible for solving numerically the equations of fluid motion governing atmospheric dynamics on the underlying grid system, includes numerous factors that can confound the Arctic climate simulation such as the choice of model grid, vertical coordinate, representation of topography, and numerical method (Ullrich et al., 2017). For example, the latitude-longitude grid system adopted by conventional atmospheric models has unique numerical modeling characteristics associated with polar regions such as pole singularity and smaller grid spaces in zonal directions at high latitude. These characteristics require models to adopt additional computational methods such as polar filter in order to stabilize their systems (Neale et al., 2012; Williamson, 2007). The fact that most atmospheric models participating in CMIP5 use the latitude-longitude grid system implies that most simulation results may be influenced by these effects.

Recent improvements in, and accumulation of, satellite and in situ observations in the Arctic have contributed to a better understanding of physical processes over the Arctic region (English et al., 2014, 2015; Hunke et al., 2010; Kay et al., 2016). Due to increasing computing resources, research has also been conducted on the strong internal variability in the Arctic region using the proper number of ensembles in the simulation of Arctic and adjacent regions (Mori et al., 2014). Although uncertainty in the physical processes is declining, the effects of dynamical cores on Arctic climate modeling have been examined less thoroughly. In particular, previous studies simply addressed possible problems of pole singularity in using a latitude-longitude grid system over the polar region (Dubos, 2009; Purser, 1988; Williamson, 2007), but the quantitative comparison of the quality of the Arctic climate simulation with other dynamic cores has not been addressed yet.

The recent development of dynamical cores using unstructured grid systems, such as cubed-sphere (Choi & Hong, 2016; Dennis et al., 2012), icosahedral grid (Zängl et al., 2015), and centroidal Voronoi mesh (Park et al., 2014), raise the necessity of evaluating the impact of existing dynamical cores on the Arctic region in global simulations. A comparison of global climate simulations between unstructured and latitude-longitude grids gives us opportunity to investigate their potential impacts on Arctic climate simulations.

This study deals with the issues raised above by comparing the Arctic climates simulated by two dynamical cores. Section 2 describes the experimental design and data, section 3 presents simulated results for the present climate and responses to sea ice reduction, and section 4 summarizes the result and discusses the possible cause and effects of dynamical cores on Arctic simulations.

## 2. Model and Data

We adopted two dynamical cores of the Community Atmosphere Model version 5 (CAM5) (Neale et al., 2012). The first was the latitude-longitude grid-based finite volume (FV) core which has been used in various climate experiments such as CMIP5 (Kay et al., 2015). The second was the cubed-sphere grid-based spectral element (SE) core which has mainly been used in CAM5. The SE core improves computational scalability with cubed-sphere grid geometries that are free from pole singularity (Dennis et al., 2012).

We carried out two sets of full-physics experiments using the FV and SE cores. First, we conducted simulations using both cores to examine the differences between present climate systems. We used sea surface temperature (SST) and sea ice conditions averaged for the period 1982–2001 (Hurrell et al., 2008), provided by the Community Earth System Model repository, as a present climate boundary condition. The physical processes in both dynamical core experiments were set to the same CAM4 physics including coefficients from the FV core's default setting. Topography was set to match the SE core.

Second, we conducted sensitivity experiments to investigate different responses to reduced sea ice by both cores. This experiment set adopts sea ice coverage north of 60°N as monthly values averaged for the period of 2001–2010, an approach used in other recent sea ice reduction simulations (Jun et al., 2016, 2014). The SST over the sea ice changed region was adjusted by statistical relationships (Jun et al., 2014). The experiments were performed for 100 years, analyzing the boreal winter (December–January–February) of the entire period.

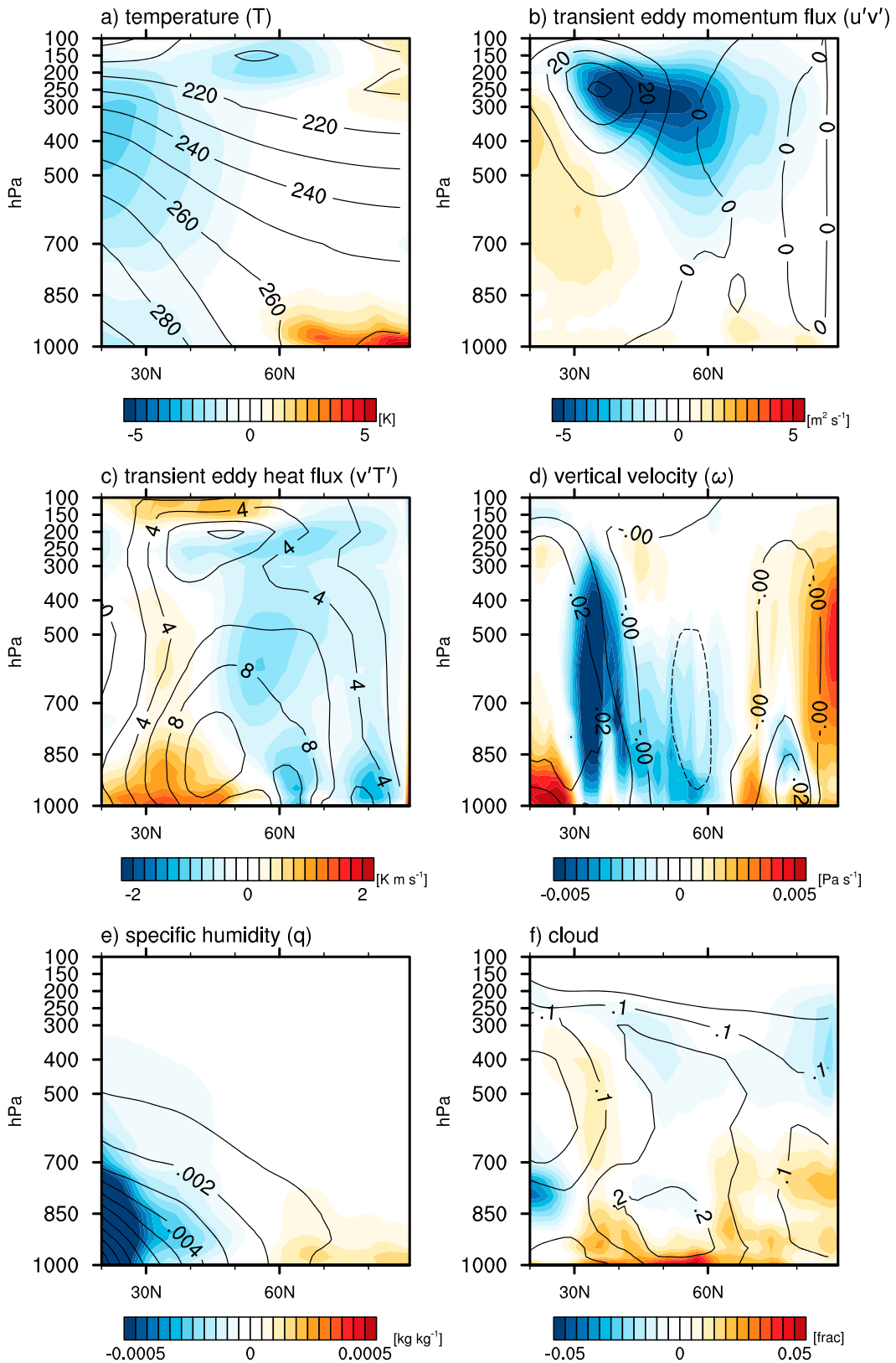


**Figure 1.** Zonally averaged climate parameters during Northern Hemisphere winter (December-January-February) produced by two full-physics climate simulations, a finite volume dynamical core (contours), and the changes produced by using a spectral element dynamical core (shading): (a) temperature, (b) transient eddy momentum flux, (c) transient eddy heat flux, (d) vertical velocity, (e) specific humidity, and (f) cloud.

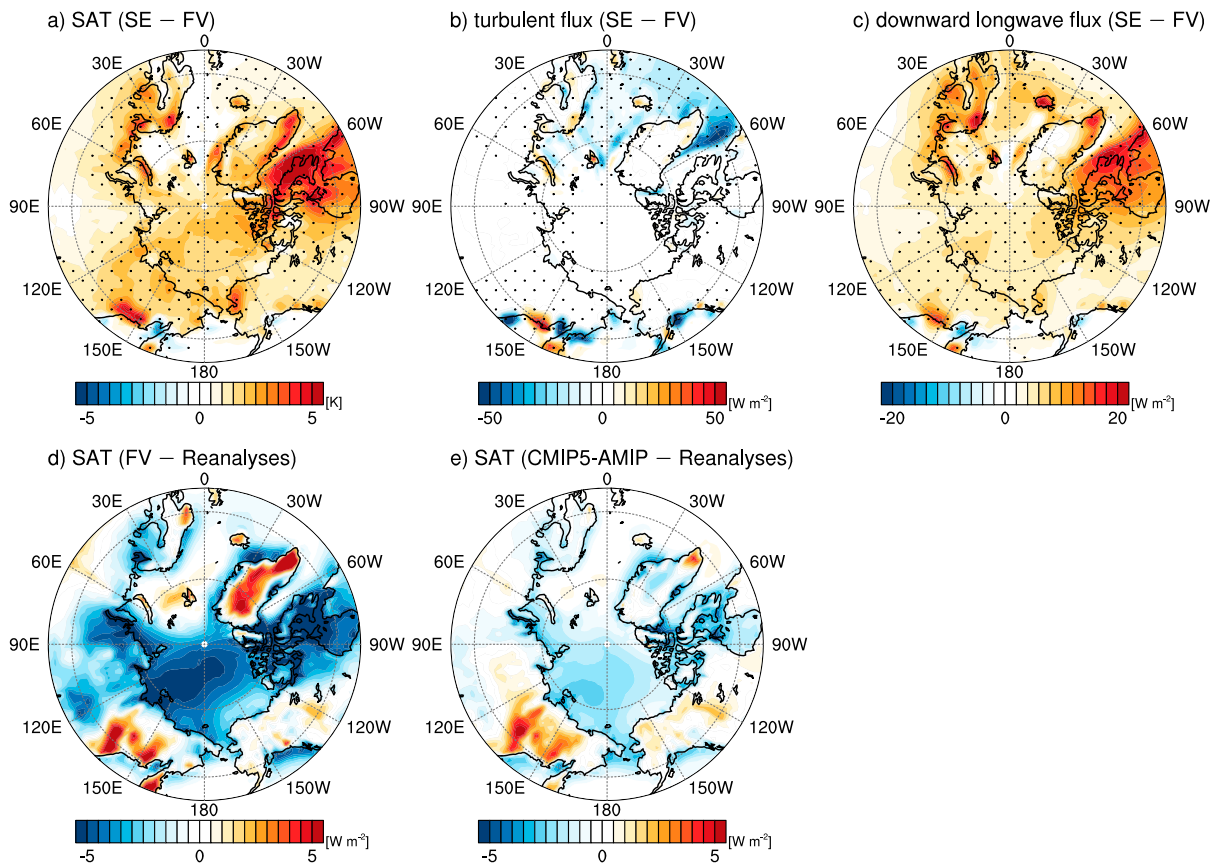


**Figure 2.** Mean simulated differences in Northern Hemisphere winter (December-January-February) between the finite volume (FV) and spectral element (SE) dynamical cores of (a) surface air temperature (SAT), (b) turbulent flux at the surface, and (c) downward longwave flux at the surface. Stippled regions indicate where the difference is significant at a 99% confidence level based on a *t* test. Winter mean SAT differences between the mean of three analyses (European Centre for Medium-Range Weather Forecasts Interim Re-Analysis, Modern-Era Retrospective Analysis for Research and Application, and National Centers for Environmental Prediction Climate Forecast System) for 1982–2001 and (d) the FV simulation and (e) a multimodel ensemble mean of 23 modeling results from the Coupled Model Intercomparison Project phase (CMIP5) historical Atmospheric Modeling Intercomparison Project (AMIP) simulation.

Horizontal resolutions for all experiments were set to about 2° at the equator for each core. The FV core uses a latitude-longitude grid system consisting of 91 latitudinal and 144 longitudinal grid points (e.g., named as fv19), while the SE core uses a cubed-sphere grid system which has six faces with 16 × 16 elements on one face and four collocation points (third-degree polynomials) on one element edge (e.g., named as ne16np4).

For comparison with modeling results, we used three reanalysis data sets: the European Centre for Medium-Range Weather Forecasts Interim Re-Analysis (Dee et al., 2011), the National Centers for Environmental Prediction Climate Forecast System Reanalysis (Saha et al., 2010), and the National Aeronautics and Space Administration Modern-Era Retrospective Analysis for Research and Application (Rienecker et al., 2011), all of which have small errors when compared to observations in the Arctic region (Lindsay et al., 2014). We also used 23 modeling results from the historical Atmospheric Modeling Intercomparison Project (AMIP) experiment from CMIP5, as discussed in section 3.

### 3. Result

The present climate experiments using the SE and FV dynamical cores showed different zonal mean temperature distributions despite using the same physical settings (Figure 1a). Compared to the FV core, the SE core simulated a colder troposphere over the subtropics and a warmer near surface over the Arctic region. Especially, warmer temperatures of more than 3 K is observed at the lower troposphere below 850 hPa north of 60°N in the SE core simulation.

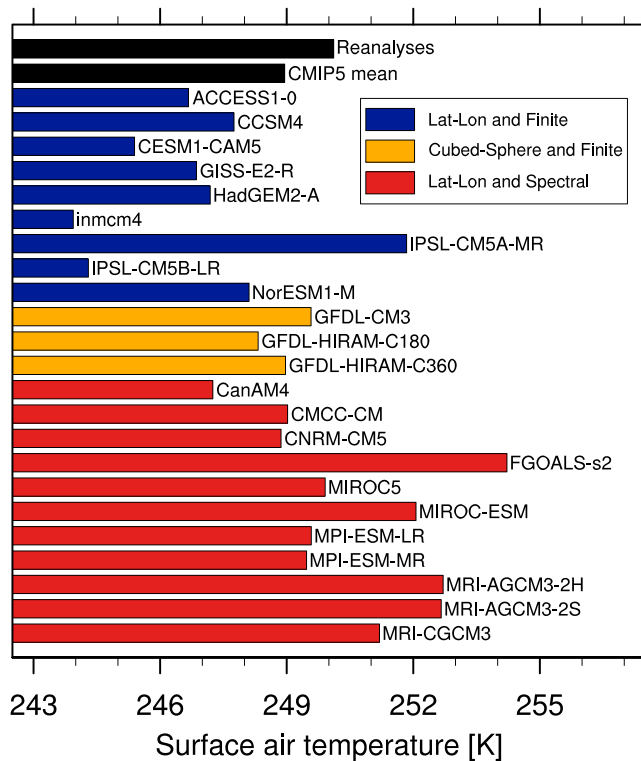


**Figure 3.** Averaged surface air temperature in winter (December-January-February) north of 65°N in historical Atmospheric Modeling Intercomparison Project simulation results from 23 Coupled Model Intercomparison Project phase 5 (CMIP5) climate models, their multimodel ensemble mean, and three reanalysis data sets (European Centre for Medium-Range Weather Forecasts Interim Re-Analysis, Modern-Era Retrospective Analysis for Research and Application, and National Centers for Environmental Prediction Climate Forecast System). Colors represent the type of grid system and dynamical core used in each model: latitude-longitude grid with finite method (dark blue), cubed-sphere grid with finite method (orange), and latitude-longitude grid with global spectral method (red).

Compared to the FV results, the surface air temperature (SAT) simulated by the SE core is about 2 K warmer across the Arctic and up to 5 K warmer northeast of the Canadian mainland (Figure 2a). However, the turbulent heat flux over Arctic regions where sea ice cover exists shows negligible differences between the two cores (Figure 2b). This demonstrates that lower tropospheric warming over the Arctic might be mainly attributed to the sinking motion described above, influenced by northward heat and moisture transport to the Arctic. The distribution of differences in downward longwave radiation between the two cores also suggests that a warm and moist lower troposphere could promote substantial near-surface warming (Figure 2c).

Focusing on the differences in distinctive winter Arctic SAT response, we compared the SAT of the two core simulations with the mean SAT of three reanalysis data sets averaged from 1982–2001; the cold tendency of SAT in the FV core is apparent (Figure 2d). The winter mean SAT north of 65°N is 247.56 K for FV, 249.44 K for SE, and 250.11 K for the average of the three reanalyses. Although both the SE and FV cores simulated colder Arctic SAT compared to the reanalyses, the largest cold difference was produced by the FV core simulation. It is notable that the multimodel mean of 23 CMIP5 simulations also tended to simulate a cold Arctic (Figure 2e), as the multimodel SAT mean over the Arctic from the CMIP5-AMIP simulations for the same period is 248.95 K, 1.16 K colder than the mean of the three reanalyses. The spatial distribution of SAT difference between CMIP5 and the reanalyses (Figure 2e) resembles that between the FV and the reanalyses (Figure 2d).

To further examine whether the Arctic surface temperature bias is systematically related to the dynamic cores in CMIP5 models, we classified the 23 CMIP5-AMIP simulations by their grid system and dynamical core type

To consider the physical processes resulting in the zonal mean temperature differences depicted in Figure 1a, we explored the possible contributions of differences in transient eddy momentum and heat fluxes and zonal mean vertical velocity between the two simulations. Figure 1b shows the difference in transient eddy momentum flux, in which the weakest momentum flux is centered at 45°N near 250 hPa in the SE simulation. This means that the weaker momentum flux induces a decrease in the momentum flux convergence ( $-\frac{\partial \overline{u'v'}}{\partial y}$ ) in this area and a weakening in the equatorward mean meridional circulation in the upper troposphere. The SE simulation also produced stronger transient eddy heat flux in the lower troposphere south of 50°N and weaker transient eddy heat flux north of 60°N (Figure 1c) compared to the FV simulation, meaning that the SE simulation tended to shift the maxima of transient eddy heat flux equatorward.

Compared to the FV simulation, the altered eddy momentum and heat fluxes of the SE simulation contributed to changes in mean circulation, producing rising motion at about 40°N and sinking motion north of 60°N in the troposphere by indirectly forced circulation (Figure 1d). The decrease in eddy momentum flux from 30°N to 45°N induced strong rising motion in the troposphere in the midlatitudes. The distribution of eddy heat flux at a positive maximum near 30°N also contributed to this indirect rising motion over the midlatitudes between 30°N and 45°N.

As a result, the SE core produced an enhanced sinking motion in the troposphere north of 60°N that enforced a warmer lower troposphere through adiabatic warming (Figure 1a). This lower tropospheric Arctic warming was also influenced by the increase in poleward eddy heat transport over the midlatitudes (Figure 1c). This increase implies that more moisture and clouds might also be transported into the Arctic near-surface region (Figures 1e and 1f). In contrast, the sinking motion south of 30°N might prevent moisture convection, leading to a drier and colder troposphere in this region (Figures 1d and 1e). Thus, the Arctic lower troposphere becomes warmer in the SE simulation compared to the FV, although the same SST and sea ice conditions were used.

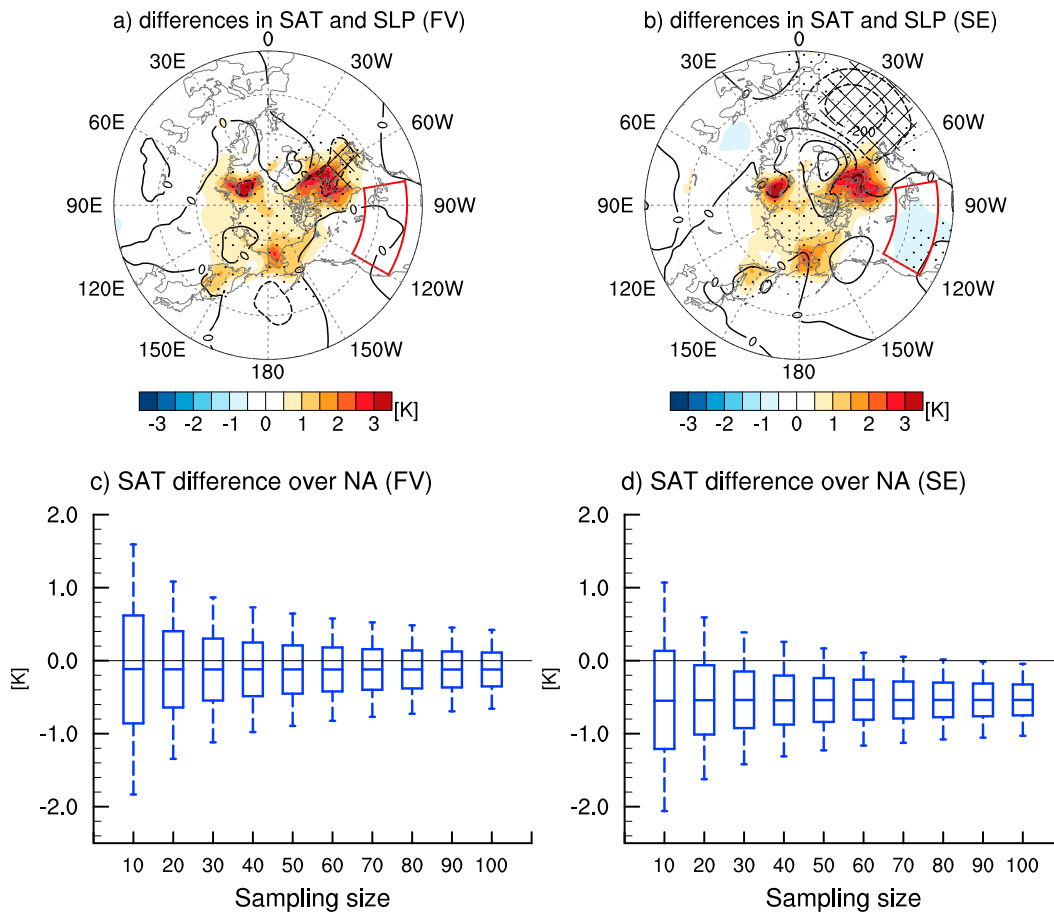


**Figure 4.** Responses of surface air temperature (SAT) and sea level pressure (SLP) to reduced sea ice over the Arctic from climate simulations conducted by (a) finite volume (FV) and (b) spectral element (SE) dynamical cores. Contour interval for SLP is 100 Pa. Stippled and cross-checked regions indicate areas where the difference is significant at the 99% confidence level based on a *t* test. Box plots show the ensemble mean SAT differences between reduced sea ice and baseline experiments for (c) the FV core and (d) the SE core averaged over North America, as defined by the red box in (a) and (b) (120–80°W, 35–55°N). Boxes and whiskers indicate ranges of one standard deviation and the 99th percentile, respectively. Box plots are estimated based on 100,000 bootstrap samples.

(Figure 3), consisting of latitude-longitude grid with finite method (e.g., finite difference and finite volume), cubed-sphere grid with finite volume method, and latitude-longitude grid with spectral method (see Table S1 in the supporting information for more detailed characteristics of the 23 CMIP5 models). The cubed-sphere grid models with finite volume method tend to simulate a moderate Arctic climate, while latitude-longitude grid models with spectral method tend to simulate a moderate-warm Arctic climate. However, all latitude-longitude grid models using finite method (except for IPSL-CM5A-MR) simulated a colder Arctic surface temperature when compared to the mean of the three reanalysis data sets and the multimodel mean of all 23 CMIP5-AMIP models. This suggests that the cold tendency of Arctic mean SAT seen in CMIP5-AMIP simulations overall originated from models adopting dynamical cores based on latitude-longitude grid with finite methods, no matter which physical processes are used. These results support our suggestion that different dynamical cores have noticeable impacts on simulation results, especially over the Arctic region.

The altered Arctic surface temperature may also lead to changes in teleconnection patterns, especially those linked to Arctic sea ice, suggesting that the choice of dynamical cores can have a remarkable effect on the remote responses of midlatitude regions with regard to reductions in sea ice. In order to examine this possibility, we compared the responses of SAT and sea level pressure (SLP) as simulated by the FV and SE cores to reduced Arctic sea ice conditions (Figure 4). Both cores showed the same pronounced warming response over the sea ice reduction region in the Arctic. In contrast, the SAT response in the midlatitude region and the SLP in the north Atlantic showed a statistically significant difference between the two cores. The FV

core produced no significant response in midlatitude SAT or northern midlatitude SLP (Figure 4a), but the SE core produced a significant cold SAT response in North America and lower pressure response in the North Atlantic (Figure 4b). Only the SE core seemed able to simulate Warm Arctic, partly Cold Continents response to reduced sea ice cover in this study.

Taking into account the strong internal variability of the winter response over the Arctic and surrounding regions, we estimated the significance of the cold response in North America using 100,000 random bootstrap samples. The SAT response over North America produced by the FV core was not significant for all ensemble sizes (Figure 4c), but the SE core's results appear robust for more than 90 ensemble sizes at a 99% confidence level (Figure 4d). This robustness with respect to the ensemble sizes is consistent with Mori et al. (2014), suggesting that there is a significant difference in midlatitude temperature responses between the FV and SE cores.

#### 4. Summary and Discussion

Our study showed that compared to the FV core on latitude-longitude grid, the SE core on cubed-sphere grid with the same physical parameterizations simulates enhanced northward heat transport in the midlatitude region and increased tropospheric sinking motion over the Arctic. In association with these dynamical processes, lower tropospheric warming over the Arctic region follows. The relatively increased sinking motion of SE in the Arctic lower atmosphere is consistent with the northward heat transport.

Various factors such as the grid system, fast-wave handling, and the physics-dynamics coupling process may contribute to this difference between eddy fluxes. Among the factors, fast-wave treatment may be profound contributors. The additional numerical filter for polar regions is a necessary requisite for models using finite method on latitude-longitude grid system (see Table S1 in the supporting information). The FV core in this study also applies an additional polar filter to stabilize fast gravity waves over high-latitude regions (Neale et al., 2012; Thatcher & Jablonowski, 2016). Although the application of the polar filter is intuitively thought to weaken the eddy fluxes by slower fast waves, in our full-physics experiments, the weakening of the upper layer momentum flux appears instead in the SE core. Further studies on the influence of the polar filter, including this counterintuitive result, are therefore needed.

Meanwhile, it should be noted that higher SAT in the SE core than in the FV core and relatively small SAT difference compared to reanalysis data sets do not mean that the SE core simulates Arctic climate more accurately than the FV core. The result of this study suggests that the SE core tends to simulate a higher SAT of the Arctic region than the FV core with only the influence of the dynamical core. In addition, the SAT over the Arctic of the reanalysis data also has inherent uncertainty due to modeling. Above all, the range of SAT simulated by the two cores can be significantly affected by the physics schemes. For example, physical processes such as sea ice thickness in the Arctic region can significantly alter the SAT over the Arctic (Lang et al., 2017). In the additional reduced sea ice thickness experiment set, the SAT difference of the FV core against reanalyses mean becomes dramatically reduced (see Figure S1 in the supporting information).

In simulations forced by reduced sea ice cover with physics settings for present climate, only the SE core simulated a robust cooling response over North America. The negligible SAT response to the reduced sea ice in FV core resembles the results of Sun et al. (2016), which demonstrates that sea ice loss does not cause cooling over the high-latitude continental regions in their multimodel ensemble. This result may be influenced by climatic conditions in the Arctic and surrounding regions simulated by different dynamical cores, as recent studies suggest that various climatic factors, such as the Pacific decadal oscillation (e.g., Screen & Francis, 2016), Atlantic multidecadal oscillation (e.g., Osborne et al., 2017), and background state of the Arctic and surrounding regions (e.g., Smith et al., 2017), contribute to the midlatitude response to warmer Arctic.

We estimate that the different stability of the lower troposphere caused by the Arctic near-surface temperature in the two cores is one of the climatic conditions that could influence the midlatitude response. Because the redistribution of Arctic surface warming can be affected by near-surface temperature inversions (Bintanja et al., 2011), a degree of cold surface over the Arctic could affect the growth of anomalous equivalent barotropic anticyclones in the vicinity of sea ice loss regions and consequently cool the downstream midlatitude regions (Kug et al., 2015). This possibility can be confirmed by the SE core simulation in which an anomalous

anticyclone over the vicinity of the Chukchi Sea was found (Figure 4b). In addition, in the artificial sea ice thickness reduction experiments of the FV core, the warmer Arctic region resulted in a cooling response in the Eurasian region as a response to sea ice reduction (see Figure S2 in the supporting information). On the other hand, in the artificial sea ice thickness reduction experiments of the SE core, SAT response in mid-latitude regions did not appear. This is presumably due to the weakening of the warming for reduced sea ice concentration in the Arctic region in these experiments.

The diversity of midlatitude responses in the two sea ice reduction experiments with the two climatic conditions in this study suggests that strong internal atmospheric variability can influence the teleconnection between the Arctic and midlatitude regions. Nonetheless, significantly different midlatitude responses between the two cores remind us that special attention should be paid to the interpretation of Arctic climate modeling results, including the results of this study, and raise the need for further studies investigating which factors in dynamical cores most affect Arctic climate simulations.

### Acknowledgments

S.-Y. Jun and B.-M. Kim are supported by "Development and Application of the Korea Polar Prediction System (KPOPS) for Climate Change and Weather Disaster (PE18130)" project of the Korea Polar Research Institute. S.-J. Choi is supported by the R&D project on the development of global numerical weather prediction systems of Korea Institute of Atmospheric Prediction Systems (KIAPS) funded by Korea Meteorological Administration (KMA). All data are freely and publicly available as follows: ERA-Interim (<http://apps.ecmwf.int/datasets>), CMIP5 (<http://esgf-node.llnl.gov/search/cmip5/>), CFSR (<https://www.ncdc.noaa.gov/data-access/model-data#cfcr>), and MERRA (<https://gmao.gsfc.nasa.gov/reanalysis/MERRA/>).

### References

- Arctic Climate Impact Assessment (2005). *Arctic: Arctic Climate Impact Assessment (ACIA)*. Cambridge, UK: Cambridge University Press.
- Bao, Q., Lin, P., Zhou, T., Liu, Y., Yu, Y., Wu, G., et al. (2013). The Flexible Global Ocean-Atmosphere-Land system model, spectral version 2: FGOALS-s2. *Advances in Atmospheric Sciences*, 30(3), 561–576. <https://doi.org/10.1007/s00376-012-2113-9>
- Bentsen, M., Bethke, I., Debernard, J. B., Iversen, T., Kirkevåg, A., Seland, Ø., et al. (2013). The Norwegian Earth System Model, NorESM1-M—Part 1: Description and basic evaluation of the physical climate. *Geoscientific Model Development*, 6(3), 687–720. <https://doi.org/10.5194/gmd-6-687-2013>
- Bi, D., Dix, M., Marsland, S. J., O'Farrell, S., Rashid, H. A., Uotila, P., et al. (2013). The ACCESS coupled model: Description, control climate and evaluation. *Australian Meteorological and Oceanographic Journal*, 63, 41–64.
- Bintanja, R., Graverson, R. G., & Hazeleger, W. (2011). Arctic winter warming amplified by the thermal inversion and consequent low infrared cooling to space. *Nature Geoscience*, 4(11), 758–761. <https://doi.org/10.1038/ngeo1285>
- Chen, J.-H., & Lin, S.-J. (2013). Seasonal predictions of tropical cyclones using a 25-km-resolution general circulation model. *Journal of Climate*, 26(2), 380–398. <https://doi.org/10.1175/JCLI-D-12-00061.1>
- Choi, S.-J., & Hong, S.-Y. (2016). A global non-hydrostatic dynamical core using the spectral element method on a cubed-sphere grid. *Asia-Pacific Journal of Atmospheric Sciences*, 52(3), 291–307. <https://doi.org/10.1007/s13143-016-0005-0>
- Davies, T., Cullen, M. J. P., Malcolm, A. J., Mawson, M. H., Staniforth, A., White, A. A., & Wood, N. (2005). A new dynamical core for the Met Office's global and regional modelling of the atmosphere. *Quarterly Journal of the Royal Meteorological Society*, 131(608), 1759–1782. <https://doi.org/10.1256/qj.04.101>
- Dee, D. P., Uppala, S. M., Simmons, A. J., Berrisford, P., Poli, P., Kobayashi, S., et al. (2011). The ERA-Interim reanalysis: Configuration and performance of the data assimilation system. *Quarterly Journal of the Royal Meteorological Society*, 137(656), 553–597. <https://doi.org/10.1002/qj.828>
- Dennis, J. M., Edwards, J., Evans, K. J., Guba, O., Lauritzen, P. H., Mirin, A. A., et al. (2012). CAM-SE: A scalable spectral element dynamical core for the Community Atmosphere Model. *International Journal of High Performance Computing Applications*, 26(1), 74–89. <https://doi.org/10.1177/1094342011428142>
- Deser, C., Terray, L., & Phillips, A. S. (2016). Forced and internal components of winter air temperature trends over North America during the past 50 years: Mechanisms and implications\*. *Journal of Climate*, 29(6), 2237–2258. <https://doi.org/10.1175/JCLI-D-15-0304.1>
- Donner, L. J., Wyman, B. L., Hemler, R. S., Horowitz, L. W., Ming, Y., Zhao, M., et al. (2011). The dynamical core, physical parameterizations, and basic simulation characteristics of the atmospheric component AM3 of the GFDL global coupled model CM3. *Journal of Climate*, 24(13), 3484–3519. <https://doi.org/10.1175/2011JCLI3955.1>
- Dubos, T. (2009). A conservative Fourier-finite-element method for solving partial differential equations on the whole sphere. *Quarterly Journal of the Royal Meteorological Society*, 135(644), 1877–1889. <https://doi.org/10.1002/qj.487>
- Dufresne, J.-L., Foujols, M.-A., Denvil, S., Caubel, A., Marti, O., Aumont, O., et al. (2013). Climate change projections using the IPSL-CM5 Earth system model: From CMIP3 to CMIP5. *Climate Dynamics*, 40(9–10), 2123–2165. <https://doi.org/10.1007/s00382-012-1636-1>
- Endo, H., Kitoh, A., Ose, T., Mizuta, R., & Kusunoki, S. (2012). Future changes and uncertainties in Asian precipitation simulated by multiphysics and multi-sea surface temperature ensemble experiments with high-resolution Meteorological Research Institute atmospheric general circulation models (MRI-AGCMs). *Journal of Geophysical Research*, 117, D16118. <https://doi.org/10.1029/2012JD017874>
- English, J. M., Gettelman, A., & Henderson, G. R. (2015). Arctic radiative fluxes: Present-day biases and future projections in CMIP5 models. *Journal of Climate*, 28(15), 6019–6038. <https://doi.org/10.1175/JCLI-D-14-00801.1>
- English, J. M., Kay, J. E., Gettelman, A., Liu, X., Wang, Y., Zhang, Y., & Chepfer, H. (2014). Contributions of clouds, surface albedos, and mixed-phase ice nucleation schemes to Arctic radiation biases in CAM5. *Journal of Climate*, 27(13), 5174–5197. <https://doi.org/10.1175/JCLI-D-13-00608.1>
- Forget, F., Hourdin, F., Fournier, R., Hourdin, C., Talagrand, O., Collins, M., et al. (1999). Improved general circulation models of the Martian atmosphere from the surface to above 80 km. *Journal of Geophysical Research*, 104(E10), 24,155–24,175. <https://doi.org/10.1029/1999JE001025>
- Hansen, J., Russell, G., Rind, D., Stone, P., Lacis, A., Lebedeff, S., et al. (1983). Efficient three-dimensional global models for climate studies: Models I and II. *Monthly Weather Review*, 111(4), 609–662. [https://doi.org/10.1175/1520-0493\(1983\)111%3C0609:ETDGMF%3E2.0.CO;2](https://doi.org/10.1175/1520-0493(1983)111%3C0609:ETDGMF%3E2.0.CO;2)
- Hines, K., Bromwich, D. H., Bai, L. S., Bitz, C. M., Powers, J. G., & Manning, K. W. (2015). Sea ice enhancements to polar WRF \*. *Monthly Weather Review*, 143(6), 2363–2385. <https://doi.org/10.1175/MWR-D-14-00344.1>
- Hodson, D. L. R., Keeley, S. P. E., West, A., Ridley, J., Hawkins, E., & Hewitt, H. T. (2013). Identifying uncertainties in Arctic climate change projections. *Climate Dynamics*, 40(11–12), 2849–2865. <https://doi.org/10.1007/s00382-012-1512-z>
- Hunke, E. C., Lipscomb, W. H., & Turner, A. K. (2010). Sea-ice models for climate study: Retrospective and new directions. *Journal of Glaciology*, 56(200), 1162–1172. <https://doi.org/10.3189/002214311796406095>

- Hurrell, J. W., Hack, J. J., Shea, D., Caron, J. M., & Rosinski, J. (2008). A new sea surface temperature and sea ice boundary dataset for the Community Atmosphere Model. *Journal of Climate*, 21(19), 5145–5153. <https://doi.org/10.1175/2008JCLI2292.1>
- Intergovernmental Panel on Climate Change (2014). In T. F. Stocker, et al. (Eds.), *Climate change 2013: The physical science basis. Contribution of Working Group I to the Fifth Assessment Report of the Intergovernmental Panel on Climate Change*. Cambridge, UK: Cambridge University Press. <https://doi.org/10.1017/CBO9781107415324>
- Jun, S.-Y., Ho, C.-H., Jeong, J.-H., Choi, Y.-S., & Kim, B.-M. (2016). Recent changes in winter Arctic clouds and their relationships with sea ice and atmospheric conditions. *Tellus A*, 68. <https://doi.org/10.3402/tellusa.v68.29130>
- Jun, S.-Y., Ho, C.-H., Kim, B.-M., & Jeong, J.-H. (2014). Sensitivity of Arctic warming to sea surface temperature distribution over melted sea-ice region in atmospheric general circulation model experiments. *Climate Dynamics*, 42(3–4), 941–955. <https://doi.org/10.1007/s00382-013-1897-3>
- Karlsson, J., & Svensson, G. (2011). The simulation of Arctic clouds and their influence on the winter surface temperature in present-day climate in the CIMP3 multi-model dataset. *Climate Dynamics*, 36(3–4), 623–635. <https://doi.org/10.1007/s00382-010-0758-6>
- Karlsson, J., & Svensson, G. (2013). Consequences of poor representation of Arctic sea-ice albedo and cloud-radiation interactions in the CIMP5 model ensemble. *Geophysical Research Letters*, 40, 4374–4379. <https://doi.org/10.1002/grl.50768>
- Kay, J. E., Bourdages, L., Miller, N. B., Morrison, A., Yettella, V., Chepfer, H., & Eaton, B. (2016). Evaluating and improving cloud phase in the Community Atmosphere Model version 5 using spaceborne lidar observations. *Journal of Geophysical Research: Atmospheres*, 121, 4162–4176. <https://doi.org/10.1002/2015JD024699>
- Kay, J. E., Deser, C., Phillips, A., Mai, A., Hannay, C., Strand, G., et al. (2015). The Community Earth System Model (CESM) large ensemble project: A community resource for studying climate change in the presence of internal climate variability. *Bulletin of the American Meteorological Society*, 96(8), 1333–1349. <https://doi.org/10.1175/BAMS-D-13-00255.1>
- Kim, B.-M., Son, S.-W., Min, S.-K., Jeong, J.-H., Kim, S.-J., Zhang, X., et al. (2014). Weakening of the stratospheric polar vortex by Arctic sea-ice loss. *Nature Communications*, 5. <https://doi.org/10.1038/ncomms5646>, 4646
- Kug, J.-S., Jeong, J.-H., Jang, Y.-S., Kim, B.-M., Folland, C. K., Min, S.-K., & Son, S.-W. (2015). Two distinct influences of Arctic warming on cold winters over North America and East Asia. *Nature Geoscience*, 8(10), 759–762. <https://doi.org/10.1038/ngeo2517>
- Lang, A., Yang, S., & Kaas, E. (2017). Sea ice thickness and recent Arctic warming. *Geophysical Research Letters*, 44, 409–418. <https://doi.org/10.1002/2016GL071274>
- Lindsay, R., Wensnahan, M., Schweiger, A., & Zhang, J. (2014). Evaluation of seven different atmospheric reanalysis products in the arctic. *Journal of Climate*, 27(7), 2588–2606. <https://doi.org/10.1175/JCLI-D-13-00014.1>
- Martin, G. M., Bellouin, N., Collins, W. J., Culverwell, I. D., Halloran, P. R., Hardiman, S. C., et al. (2011). The HadGEM2 family of Met Office Unified Model climate configurations. *Geoscientific Model Development*, 4(3), 723–757. <https://doi.org/10.5194/gmd-4-723-2011>
- Meehl, G. A., Washington, W. M., Arblaster, J. M., Hu, A., Teng, H., Kay, J. E., et al. (2013). Climate change projections in CESM1(CAM5) compared to CCSM4. *Journal of Climate*, 26(17), 6287–6308. <https://doi.org/10.1175/JCLI-D-12-00572.1>
- Meehl, G. A., Washington, W. M., Arblaster, J. M., Hu, A., Teng, H., Tebaldi, C., et al. (2012). Climate system response to external forcings and climate change projections in CCSM4. *Journal of Climate*, 25(11), 3661–3683. <https://doi.org/10.1175/JCLI-D-11-00240.1>
- Mizuta, R., Yoshimura, H., Murakami, H., Matsueda, M., Endo, H., Ose, T., et al. (2012). Climate simulations using MRI-AGCM3.2 with 20-km grid. *Journal of the Meteorological Society of Japan. Ser. II*, 90A, 233–258. <https://doi.org/10.2151/jmsj.2012-A12>
- Mori, M., Watanabe, M., Shiogama, H., Inoue, J., & Kimoto, M. (2014). Robust Arctic sea-ice influence on the frequent Eurasian cold winters in past decades. *Nature Geoscience*, 7(12), 869–873. <https://doi.org/10.1038/ngeo2277>
- Neale, R. B., Chen, C.-C., Gettelman, A., Lauritzen, P. H., Park, S., Williamson, D. L., et al. (2012). Description of the NCAR community atmosphere model (CAM 5.0). NCAR Tech. Note NCAR/TN-486+ STR. Boulder, CO: National Center for Atmospheric Research.
- Osborne, J. M., Screen, J. A., & Collins, M. (2017). Ocean–atmosphere state dependence of the atmospheric response to Arctic sea ice loss. *Journal of Climate*, 30(5), 1537–1552. <https://doi.org/10.1175/JCLI-D-16-0531.1>
- Overland, J. E., Dethloff, K., Francis, J. A., Hall, R. J., Hanna, E., Kim, S.-J., et al. (2016). Nonlinear response of mid-latitude weather to the changing Arctic. *Nature Climate Change*, 6(11), 992–999. <https://doi.org/10.1038/nclimate3121>
- Overland, J. E., Wood, K. R., & Wang, M. (2011). Warm Arctic—Cold continents: Climate impacts of the newly open Arctic Sea. *Polar Research*, 30(1), 15787. <https://doi.org/10.3402/polar.v30i0.15787>
- Park, S.-H., Klemp, J. B., & Skamarock, W. C. (2014). A comparison of mesh refinement in the global MPAS-A and WRF models using an idealized normal-mode baroclinic wave simulation. *Monthly Weather Review*, 142(10), 3614–3634. <https://doi.org/10.1175/MWR-D-14-00004.1>
- Purser, J. (1988). Degradation of numerical differencing caused by Fourier filtering at high latitudes. *Monthly Weather Review*, 116(5), 1057–1066. [https://doi.org/10.1175/1520-0493\(1988\)116%3C1057:DONDCB%3E2.0.CO;2](https://doi.org/10.1175/1520-0493(1988)116%3C1057:DONDCB%3E2.0.CO;2)
- Putman, W. M., & Lin, S.-J. (2007). Finite-volume transport on various cubed-sphere grids. *Journal of Computational Physics*, 227(1), 55–78. <https://doi.org/10.1016/J.JCP.2007.07.022>
- Rampal, P., Weiss, J., Dubois, C., & Campin, J.-M. (2011). IPCC climate models do not capture Arctic sea ice drift acceleration: Consequences in terms of projected sea ice thinning and decline. *Journal of Geophysical Research*, 116, C00D07. <https://doi.org/10.1029/2011JC007110>
- Randall, D., Curry, J., Battisti, D., Flato, G., Grumbine, R., Hakkinen, S., et al. (1998). Status of and outlook for large-scale modeling of atmosphere–ice–ocean interactions in the Arctic. *Bulletin of the American Meteorological Society*, 79(2), 197–219. [https://doi.org/10.1175/1520-0477\(1998\)079%3C0197:SOAOF%3E2.0.CO;2](https://doi.org/10.1175/1520-0477(1998)079%3C0197:SOAOF%3E2.0.CO;2)
- Rienecker, M. M., Suarez, M. J., Gelaro, R., Todling, R., Bacmeister, J., Liu, E., et al. (2011). MERRA: NASA's Modern-Era Retrospective Analysis for Research and Applications. *Journal of Climate*, 24(14), 3624–3648. <https://doi.org/10.1175/JCLI-D-11-00015.1>
- Saha, S., Moorthi, S., Pan, H.-L., Wu, X., Wang, J., Nadiga, S., et al. (2010). The NCEP climate forecast system reanalysis. *Bulletin of the American Meteorological Society*, 91(8), 1015–1058. <https://doi.org/10.1175/2010BAMS3001.1>
- Schmidt, G. A., Kelley, M., Nazarenko, L., Ruedy, R., Russell, G. L., Aleinov, I., et al. (2014). Configuration and assessment of the GISS ModelE2 contributions to the CIMP5 archive. *Journal of Advances in Modeling Earth Systems*, 6, 141–184. <https://doi.org/10.1002/2013MS000265>
- Scoccimarro, E., Gualdi, S., Bellucci, A., Sanna, A., Giuseppe Fogli, P., Manzini, E., et al. (2011). Effects of tropical cyclones on ocean heat transport in a high-resolution coupled general circulation model. *Journal of Climate*, 24(16), 4368–4384. <https://doi.org/10.1175/2011JCLI4104.1>
- Screen, J. A., & Francis, J. A. (2016). Contribution of sea-ice loss to Arctic amplification is regulated by Pacific Ocean decadal variability. *Nature Climate Change*, 6, 856. <https://doi.org/10.1038/nclimate3011>
- Smith, D. M., Dunstone, N. J., Scaife, A. A., Fiedler, E. K., Copsey, D., & Hardiman, S. C. (2017). Atmospheric response to Arctic and Antarctic sea ice: The importance of ocean–atmosphere coupling and the background state. *Journal of Climate*, 30(12), 4547–4565. <https://doi.org/10.1175/JCLI-D-16-0564.1>

- Stevens, B., Giorgetta, M., Esch, M., Mauritsen, T., Crueger, T., Rast, S., et al. (2013). Atmospheric component of the MPI-M Earth System Model: ECHAM6. *Journal of Advances in Modeling Earth Systems*, 5, 146–172. <https://doi.org/10.1002/jame.20015>
- Stroeve, J. C., Kattsov, V., Barrett, A., Serreze, M., Pavlova, T., Holland, M., & Meier, W. N. (2012). Trends in Arctic sea ice extent from CMIP5, CMIP3 and observations. *Geophysical Research Letters*, 39, L16502. <https://doi.org/10.1029/2012GL052676>
- Stroeve, J. C., Serreze, M. C., Holland, M. M., Kay, J. E., Malanik, J., & Barrett, A. P. (2012). The Arctic's rapidly shrinking sea ice cover: A research synthesis. *Climatic Change*, 110(3-4), 1005–1027. <https://doi.org/10.1007/s10584-011-0101-1>
- Sun, L., Perlwitz, J., & Hoerling, M. (2016). What caused the recent “Warm Arctic, Cold Continents” trend pattern in winter temperatures? *Geophysical Research Letters*, 43, 5345–5352. <https://doi.org/10.1002/2016GL069024>
- Thatcher, D. R., & Jablonowski, C. (2016). A moist aquaplanet variant of the Held–Suarez test for atmospheric model dynamical cores. *Geoscientific Model Development*, 9(4), 1263–1292. <https://doi.org/10.5194/gmd-9-1263-2016>
- Ullrich, P. A., Jablonowski, C., Kent, J., Lauritzen, P. H., Nair, R., Reed, K. A., et al. (2017). DCMIP2016: A review of non-hydrostatic dynamical core design and intercomparison of participating models. *Geoscientific Model Development*, 10(12), 4477–4509. <https://doi.org/10.5194/gmd-10-4477-2017>
- Van Oldenborgh, G. J., Haarsma, R., De Vries, H., & Allen, M. R. (2015). Cold extremes in North America vs. mild weather in Europe: The winter of 2013–14 in the context of a warming world. *Bulletin of the American Meteorological Society*, 96(5), 707–714. <https://doi.org/10.1175/BAMS-D-14-00036.1>
- Vavrus, S., & Waliser, D. (2008). An improved parameterization for simulating Arctic cloud amount in the CCSM3 climate model. *Journal of Climate*, 21(21), 5673–5687. <https://doi.org/10.1175/2008JCLI2299.1>
- Vavrus, S., Waliser, D., Schweiger, A., & Francis, J. (2009). Simulations of 20th and 21st century Arctic cloud amount in the global climate models assessed in the IPCC AR4. *Climate Dynamics*, 33(7–8), 1099–1115. <https://doi.org/10.1007/s00382-008-0475-6>
- Voldoire, A., Sanchez-Gomez, E., y Méliá, D., Decharme, B., Cassou, C., Sénési, S., et al. (2013). The CNRM-CM5.1 global climate model: Description and basic evaluation. *Climate Dynamics*, 40(9–10), 2091–2121. <https://doi.org/10.1007/s00382-011-1259-y>
- Volodin, E. M., Dianskii, N. A., & Gusev, A. V. (2010). Simulating present-day climate with the INMCM4.0 coupled model of the atmospheric and oceanic general circulations. *Izvestiya Atmospheric and Oceanic Physics*, 46(4), 414–431. <https://doi.org/10.1134/S000143381004002X>
- von Salzen, K., Scinocca, J. F., McFarlane, N. A., Li, J., Cole, J. N. S., Plummer, D., et al. (2013). The Canadian fourth generation atmospheric global climate model (CanAM4). Part I: Representation of physical processes. *Atmosphere-Ocean*, 51(1), 104–125. <https://doi.org/10.1080/07055900.2012.755610>
- Wallace, J. M., Held, I. M., Thompson, D. W. J., Trenberth, K. E., & Walsh, J. E. (2014). Global warming and winter weather. *Science*, 343(6172), 729–730. <https://doi.org/10.1126/science.343.6172.729>
- Walsh, J. E., Fetterer, F., Scott Stewart, J., & Chapman, W. L. (2017). A database for depicting Arctic sea ice variations back to 1850. *Geographical Review*, 107(1), 89–107. <https://doi.org/10.1111/j.1931-0846.2016.12195.x>
- Walsh, J. E., Kattsov, V. M., Chapman, W. L., Govorkova, V., & Pavlova, T. (2002). Comparison of Arctic climate simulations by uncoupled and coupled global models. *Journal of Climate*, 15(12), 1429–1446. [https://doi.org/10.1175/1520-0442\(2002\)015%3C1429:COACSB%3E2.0.CO;2](https://doi.org/10.1175/1520-0442(2002)015%3C1429:COACSB%3E2.0.CO;2)
- Watanabe, S., Hajima, T., Sudo, K., Nagashima, T., Takemura, T., Okajima, H., et al. (2011). MIROC-ESM 2010: Model description and basic results of CMIP5-20c3m experiments. *Geoscientific Model Development*, 4(4), 845–872. <https://doi.org/10.5194/gmd-4-845-2011>
- Watanabe, M., Suzuki, T., Oishi, R., Komuro, Y., Watanabe, S., Emori, S., et al. (2010). Improved climate simulation by MIROC5: Mean states, variability, and climate sensitivity. *Journal of Climate*, 23(23), 6312–6335. <https://doi.org/10.1175/2010JCLI3679.1>
- Williamson, D. L. (2007). The evolution of dynamical cores for global atmospheric models. *Journal of the Meteorological Society of Japan*, 85B, 241–269. <https://doi.org/10.2151/jmsj.85B.241>
- Yao, Y., Huang, J., Luo, Y., & Zhao, Z. (2016). Improving the WRF model's (version 3.6.1) simulation over sea ice surface through coupling with a complex thermodynamic sea ice model (HIGHTSI). *Geoscientific Model Development*, 9(6), 2239–2254. <https://doi.org/10.5194/gmd-9-2239-2016>
- Yukimoto, S., Adachi, Y., Hosaka, M., Sakami, T., Yoshimura, H., Hirabara, M., et al. (2012). A new global climate model of the meteorological research institute: MRI-CGCM3—Model description and basic performance. *Journal of the Meteorological Society of Japan. Ser. II*, 90A(0), 23–64. <https://doi.org/10.2151/jmsj.2012-A02>
- Zängl, G., Reinert, D., Ripodas, P., & Baldauf, M. (2015). The ICON (ICOsahedral non-hydrostatic) modelling framework of DWD and MPI-M: Description of the non-hydrostatic dynamical core. *Quarterly Journal of the Royal Meteorological Society*, 141(687), 563–579. <https://doi.org/10.1002/qj.2378>
- Zhao, M., Held, I. M., Lin, S.-J., & Vecchi, G. A. (2009). Simulations of global hurricane climatology, interannual variability, and response to global warming using a 50-km resolution GCM. *Journal of Climate*, 22(24), 6653–6678. <https://doi.org/10.1175/2009JCLI3049.1>